Growth of $Sr_6Rh_5O_{15}$ Single Crystals from High-Temperature Solutions: Structure Determination Using the Traditional 3-D and the 4-D Superspace Group Methods and Magnetic Measurements on Oriented Single Crystals

Katharine E. Stitzer,[†] Ahmed El Abed,[‡,§] Jacques Darriet,*[,‡] and Hans-Conrad zur Loye*[,†]

Department of Chemistry and Biochemistry, University of South Carolina, Columbia, South Carolina 29208, and Institut de Chimie de la Matière Condensée de Bordeaux (ICMCB-CNRS), Avenue du Dr. Schweitzer, 33608 Pessac Cedex, France

Received April 27, 2001

Abstract: Single crystals of $Sr_6Rh_5O_{15}$ were grown from a molten potassium carbonate flux. The structure was solved by both the traditional 3-D crystallographic approach and the 4-D superspace group approach using JANA2000. Both methods produced an equivalent structure determination, thereby confirming the 4-D superspace group approach as an effective structure solution method for 3-D commensurate composite structures. $Sr_6Rh_5O_{15}$ corresponds to the $n = 1$, $m = 1$ member of the $A_{3n+3m}A'_nB_{3m+n}O_{9m+6n}$ family of 2H hexagonal perovskite-related oxides. This compound is characterized by pseudo-one-dimensional polyhedral chains of four face-sharing RhO_6 octahedra followed by one RhO_6 trigonal prism. These chains in turn are separated by $[Sr]_\infty$ chains. Magnetic measurements were carried out on oriented single crystals, and a very large magnetic anisotropy in the magnetic susceptibility was observed.

Introduction

Low-dimensional magnetic systems have attracted much interest historically due to the presence of magnetic behavior unique to structurally anisotropic systems.[1−3] This structural anisotropy can in turn give rise to a corresponding anisotropy in the electronic and magnetic properties of such materials. If a single crystal is available, such properties can be measured as a function of the physical orientation of the crystal relative to the measurement direction. Consequently, the ability to grow large high-quality single crystals is greatly valued, as one can readily detect, measure, and quantify existing electronic and magnetic anisotropies using single crystals.

During the past years, our group has succeeded in using carbonate fluxes to grow very large, high-quality, single crystals of 2H-perovskite-related oxides,[4−6] which has made possible precise structural determination of a number of these compounds. Equally important, however, these single crystals have now enabled us to investigate the magnetic behavior of these oxides as a function of crystal orientation relative to an applied magnetic field. In this paper, we discuss both the structure determination and the magnetic properties of $Sr_6Rh_5O_{15}$, a member of a larger family of oxides of general composition $A_{3n+3m}A'_nB_{3m+n}O_{9m+6n}$.

Our group is one of several that have been investigating the structures and magnetic properties of a family of low-dimensional oxides, $A_{3n+3m}A'_nB_{3m+n}O_{9m+6n}$ (n, m = integers, A = alkaline earth; A′, B = large assortment of metals including alkali, alkaline earth, transition, main group, and rare earth metals),[7−28] that are structurally closely related to the 2H hexagonal perovskites. These complex oxides contain chains

* To whom correspondence should be addressed. E-mail: zurloye@sc.edu.
† University of South Carolina.
‡ Institut de Chimie de la Matière Condensée de Bordeaux.
§ Permanent address: Facultédes Sciences, Mohamed I University, Oujda, Morocco.

(1) Schlenker, C.; Dumas, J. In *Crystal Chemistry and Properties of Materials with Quasi-One-Dimensional Structures, a Chemical and Physical Approach*; Rouxel, J., Ed.; Reidel Publishing Co.: Boston, 1986; p 135.
(2) de Jongh, L. J.; Miedema, A. R. *Adv. Phys.* **1974**, *23*, 1.
(3) Day, P. In *Solid State Chemistry Compounds*; Cheetham, A. K., Day, P., Eds.; Clarendon Press: Oxford, U.K., 1992; Chapter 2.
(4) Claridge, J. B.; Layland, R. C.; Henley, W. H.; zur Loye, H.-C. *Chem. Mater.* **1999**, *11*, 1376.
(5) Henley, W. H.; Claridge, J. B.; Smallwood, P. L.; zur Loye, H.-C. *J. Cryst. Growth* **1999**, *204*, 122.
(6) zur Loye, H.-C.; Layland, R. C.; Smith, M. D.; Claridge, J. B. *J. Cryst. Growth* **2000**, *211*, 452.
(7) Nguyen, T. N.; Giaquinta, D. M.; zur Loye, H.-C. *Chem. Mater.* **1994**, *6*, 1642.
(8) Nguyen, T. N.; Lee, P. A.; zur Loye, H.-C. *Science* **1996**, *271*, 489.
(9) Fjellvag, H.; Gulbrandsen, E.; Aasland, S.; Olsen, A.; Hauback, B. C. *J. Solid State Chem.* **1996**, *124*, 190.
(10) Kageyama, H.; Yoshimura, K.; Kosuge, K.; Mitamura, H.; Goto, T. *J. Phys. Soc. Jpn.* **1997**, *66*, 1607.
(11) Campa, J. A.; Gutierrez-Puebla, E.; Monge, M. A.; Rasines, I.; Ruiz-Valero, C. *J. Solid State Chem.* **1994**, *108*, 230.
(12) Harrison, W. T. A.; Hegwood, S. L.; Jacobson, A. J. *J. Chem. Soc., Chem. Commun.* **1995**, 1953.
(13) Battle, P. D.; Blake, G. R.; Darriet, J.; Gore, J. G.; Weill, F. *J. Mater. Chem.* **1997**, *7*, 1559.
(14) Strunk, M.; Muller-Buschbaum, H. J. *Alloys Compd.* **1994**, *209*, 189.
(15) Dussarrat, C.; Fompeyrine, J.; Darriet, J. *Eur. J. Solid State Inorg. Chem.* **1995**, *32*, 3.
(16) Campa, J. A.; Gutierrez-Puebla, E.; Monge, A.; Rasines, I.; Ruiz-Valero, C. *J. Solid State Chem.* **1996**, *126*, 27.
(17) Claridge, J. B.; Layland, R. C.; Adams, R. D.; zur Loye, H.-C. Z. *Anorg. Allg. Chem.* **1997**, *623*, 1131.
(18) Reisner, B. A.; Stact, A. M. *J. Am. Chem. Soc.* **1998**, *120*, 9682.
(19) Blake, G. R.; Sloan, J.; Vente, J. F.; Battle, P. D. *Chem. Mater.* **1998**, *10*, 3536.
(20) Huve, M.; Renard, C.; Abraham, F.; Van Tendeloo, G.; Amelinckx, S. *J. Solid State Chem.* **1998**, *135*, 1.
(21) Boulahya, K.; Parras, M.; Gonzalez-Calbet, J. M. *J. Solid State Chem.* **1999**, *142*, 419.
(22) Smith, M. D.; zur Loye, H.-C. *Chem. Mater.* **2000**, *12*, 2404.

10.1021/ja011071g CCC: $20.00
Published on Web 08/15/2001

of transition metals consisting of BO_6 octahedra and $A'O_6$ trigonal prisms sharing faces along the *c*-axis of the hexagonal unit cell. As a group, these oxides can be considered to represent a structural continuum between the 2H-perovskite structure of $BaNiO_3$[29] and the K_4CdCl_6 structure of Sr_4PtO_6.[30] An early general structural classification of these materials based on the filling of interstitial sites generated by the stacking of $m[A_3O_9]$ and $n[A_3A'O_6]$ layers was developed by Darriet and Subramanian.[31,32] This approach easily describes the structural composition of all the commensurate members of this family of structures and can be extended to encompass members that form incommensurately modulated (aperiodic) structures.

A general formula for this oxide family has been expressed in an equivalent way as $A_{1+x}(A'_xB_{1-x})O_3$, where the composition variable *x* can be envisaged to be any number between 0 and $^1/_2$.[33] The ratio of prisms and octahedra in the chains is determined by the ratio of A′ atoms to B atoms, that is $N_{prisms}/N_{octahedra} = x/(1 - x)$. A more unifying picture is obtained if the compounds are described as modulated composite structures.[24,32−35] Detailed explanation of the composite structure approach and its description using the superspace formalism can be found in the following papers, refs 36−40 and references therein.

For this family of oxides, the structure is best depicted as two mutually interacting subsystems,[24,32−35] modulated along *z* but periodic on the *xy* plane. The first subsystem (1) consists of [(A′, B)O_3] chains with an average *c*-lattice parameter c_1 close to $c_{perov}/2$ (c_{perov} = *c*-parameter of 2H hexagonal perovskite). The other subsystem (2) is formed by the A cations and has a *c*-lattice parameter $c_2 = c_{perov}$. Therefore, the composition of a given compound is directly related to the γ-value $= c_2^*/c_1^* = c_1/c_2$ by the relation $\gamma = (1 + x)/2$.[32,33] The γ-parameter can vary between 0.5 and 0.75 corresponding to the range of values of x ($0 \le x \le 0.5$) or equivalently corresponding to the $BaNiO_3$ and Sr_4PtO_6 structures, respectively. The structure of a compound $A_{1+x}(A'_xB_{1-x})O_3$ is commensurate if *x* is a rational value and can be matched exactly to a fraction *p*/*k* but formally incommensurate only if *x* has an irrational value. Yet, any experimental value of γ (or *x*) can be matched within experimental resolution, to some fraction *p*/*k*. Therefore, the composite, in these cases, is formally commensurate with a superstructure unit cell parameter $c_s = c_1k = c_2p$. In practice, however, an incommensurate approximation can be valid for any fraction *p*/*k* with large value of *k*.[39]

Using this formalism, it is possible to solve a *commensurate* structure by either the classical single-crystal structure solution approach, where a unit cell and the corresponding atomic positions are determined or, alternatively, in this crystal system, a superspacegroup formalism that takes advantage of the composite nature of these structures, where a small number of atomic positions and the corresponding occupational and displacive modulations are determined. Both methods are applicable, and in this paper, we demonstrate that the same structure is obtained from both methods using a recently grown single crystal of $Sr_6Rh_5O_{15}$ as an example.

We previously reported on the structure of $Sr_6Rh_5O_{15}$, an $n = 1$, $m = 1$ member of this family, determined using powder X-ray diffraction data only.[41] This analysis let us propose a structural model that was closely related to the $Ba_6Ni_5O_{15}$[11] structure; a doubled *a*-axis was invoked to account for all the observed X-ray diffraction peaks. More recently, Gonzalez-Calbet and co-workers[42] reported on a TEM study of a similar powdered $Sr_6Rh_5O_{15}$ (nominal composition) material, for which they reported a rhombohedral unit cell that is a superstructure of the $Ba_6Ni_5O_{15}$ structure. The superstructure, according to them, is due to the existence of rhodium vacancies in the form of unoccupied trigonal prismatic sites. These vacancies change the composition from $Sr_6Rh_5O_{15}$ to $Sr_6Rh_{4.4}O_{15}$, a composition confirmed by microprobe. Clearly, it is not reasonable to compare $Sr_6Rh_5O_{15}$ to $Sr_6Rh_{4.4}O_{15}$, as the rhodium content is not the same, and not surprisingly, the structures are different. In this paper, we report the single-crystal structure determination of a crystal having the ideal composition $Sr_6Rh_5O_{15}$ solved both by the superspacegroup formalism and by the standard 3-D crystallographic method. The data show conclusively that the structure of stoichiometric $Sr_6Rh_5O_{15}$ contains no rhodium vacancies and is, in fact, isostructural with $Ba_6Ni_5O_{15}$. The two independent structure solutions obtained by the 3-D and the 4-D approach demonstrates very nicely the equivalency of the two structure solution approaches. Furthermore, we present magnetic measurements of aligned single crystals of $Sr_6Rh_5O_{15}$ and report on the very large magnetic anisotropy that is observed.

Experimental Section

Crystal Growth. Rh powder (0.1544 g, 1.5 mmol; Engelhard, 99.5%), $SrCO_3$ (1.5501 g, 10.5 mmol; Alfa, 99.99%), and K_2CO_3 (17.1 g, 130 mmol; Fisher, reagent grade) were mixed thoroughly and placed in an alumina crucible. The filled crucible was covered and heated in air from room temperature to the reaction temperature of 1050 °C at 600 h^{-1}, held at 1050 °C for 48 h, and cooled to room temperature by turning off the furnace. The flux was removed with water, and the crystals were isolated manually.

Scanning Electron Microscopy. Scanning electron micrographs of several single-crystal samples were obtained using a Hitachi 2500 Delta SEM instrument. The crystals were sputtered with carbon to prevent charging. An SEM image of a typical crystal is shown in Figure 1. The SEM also verified the presence of only Sr and Rh in all crystals.

Magnetic Susceptibility. Magnetic susceptibility of powder samples of $Sr_6Rh_5O_{15}$ as a function of temperature was measured using a Quantum Design MPMS XL SQUID magnetometer, at an applied field strength of 5 kG. Both field-cooled (FC) and zero-field cooled (ZFC) measurements were performed, in the temperature range $2\ K \le T \le 300\ K$. The sample was contained in a gelatin capsule fastened in a plastic straw for immersion into the SQUID. No diamagnetic correction was needed for the sample container.

(23) Irons, S. H.; Sangrey, T. D.; Beauchamp, K. M.; Smith, M. D.; zur Loye, H.-C. *Phys. Rev. B* **2000**, *61*, 11594.
(24) Zakhour-Nakhl, M.; Claridge, J. B.; Darriet, J.; Weill, F.; zur Loye, H.-C.; Perez-Mato, J. M. *J. Am. Chem. Soc.* **2000**, *122*, 1618.
(25) Layland, R. C.; zur Loye, H.-C. *J. Alloys Compd.* **2000**, *299*, 118.
(26) Layland, R. C.; Kirkland, S. L.; zur Loye, H.-C. *J. Solid State Chem.* **1998**, *139*, 79.
(27) Smith, M. D.; Stalick, J. K.; zur Loye, H.-C. *Chem. Mater.* **1999**, *11*, 2984.
(28) Moore, C. A.; Cussen, E. J.; Battle, P. D. *J. Solid State Chem.* **2000**, *153*, 254.
(29) Lander, J. J. *Acta Crystallogr.* **1951**, *4*, 148.
(30) Randall, J. J.; Katz, L. *Acta Crystallogr.* **1959**, *12*, 519.
(31) Darriet, J.; Subramanian, M. A. *J. Mater. Chem.* **1995**, *5*, 543.
(32) Perez-Mato, J. M.; Zakhour-Nakhl, M.; Weill, F.; Darriet, J. *J. Mater. Chem.* **1999**, *9*, 2795.
(33) Evain, M.; Boucher, F.; Gourdon, O.; Petricek, V.; Dusek, M.; Bezdicka, P. *Chem. Mater.* **1998**, *10*, 3068.
(34) Ukei, K.; Yamamoto, A.; Watanabe, Y.; Shishido, T.; Fukuda, T. *Acta Crystallogr.* **1993**, *B49*, 67.
(35) Zakhour-Nakhl, M.; Weill, F.; Darriet, J.; Perez-Mato, J. M. *Inter. J. Inorg. Mater.* **2000**, *2*, 71.
(36) van Smaalen, S. *Phys. Rev. B* **1991**, *43*, 11330.
(37) Janner, A.; Janssen, T. *Acta Crystallogr.* **1980**, *A36*, 399.
(38) Janner, A.; Janssen, T. *Acta Crystallogr.* **1980**, *A36*, 408.
(39) Perez-Mato, J. M.; Madariaga, G.; Zuniga, F. J.; Garcia Arribas, A. *Acta Crystallogr.* **1987**, *A43*, 216.
(40) van Smaalen, S. *Cryst. Rev.* **1995**, *4*, 79.
(41) Claridge, J. B.; zur Loye, H.-C. *Chem. Mater.* **1998**, *10*, 2320.
(42) Varela, A.; Boulahya, K.; Parras, M.; Gonzalez-Calbet, J. M. *Chem. Mater.* **2000**, *12*, 3237.

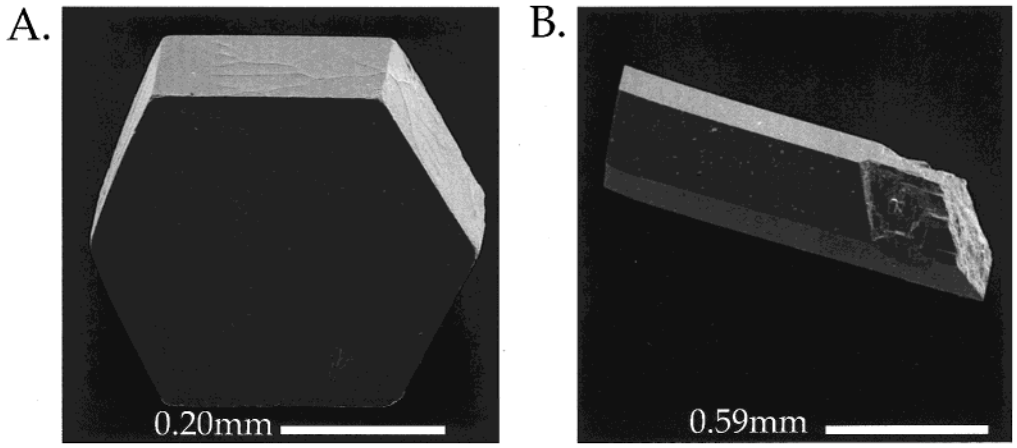

Figure 1. Flux-grown single crystals of $Sr_6Rh_5O_{15}$. (A) A typical crystal used for the structure determination. (B) A longer rodlike crystal typical of those used for aligned magnetic measurements.

Aligned single-crystal measurements were performed using a Quantum Design single-crystal rotator attachment. A large single crystal was affixed to the crystal rotator using standard vacuum grease and immersed in the SQUID magnetometer. The crystal rotator enables continuous in situ measurements of magnetization as a function of crystal orientation relative to the applied field. After centering the crystal in the instrument, the susceptibility was measured as a function of crystal orientation. The crystal is rotated in 10° steps through 360°. Knowing the initial orientation of the crystal makes it possible to determine whether the maximum or minimum susceptibility position corresponds to the *c*-axis of the crystal being oriented parallel or perpendicular to the applied magnetic field. To determine the temperature dependence of the susceptibility, the crystal position is set to correspond to either the maximum or the minimum susceptibility position. With the position fixed, the susceptibility is then measured as a function of temperature. This procedure is repeated for both the parallel and the perpendicular crystal orientations.

Data Collection. Data collection was performed on an Enraf-Nonius Kappa CCD diffractometer. The time of measurement was 10 s/frame, and the scan angle was 2°. The distance between the single crystal and the detector was fixed at 30 mm. The maximum value of θ was 30° ($(\sin\theta/\lambda)_{max} = 0.7$). A total of 11 725 reflections were measured for a redundancy fixed at 1.5 giving rise to 648 independent reflections (*R*32 space group).

Measured intensities were corrected for Lorentz and polarization effects. Absorption corrections were applied by using the Gaussian method. Additional crystallographic data and collection information are summarized in Table 1. The transformation of the 3-D indices to (3 + 1)D *hklm* values was performed by the JANA2000 program package.[43] The two subsystems, $[(Rh,Rh')O_3]_\infty$ and $[Sr]_\infty$, are modulated with respect to each other and the subsystem $[(Rh,Rh')O_3]_\infty$ was chosen as the reference. The first and second subsystem reflections sets are obtained from the (3 + 1)D superspace reflection indices by the application of the $\mathbf{W}^1$ and $\mathbf{W}^2$ transformation matrices, respectively:[36]

$$\mathbf{W}^1 = \begin{vmatrix} 1 & 0 & 0 & 0 \\ 0 & 1 & 0 & 0 \\ 0 & 0 & 1 & 0 \\ 0 & 0 & 0 & 1 \end{vmatrix} \mathbf{W}^2 = \begin{vmatrix} 1 & 0 & 0 & 0 \\ 0 & 1 & 0 & 0 \\ 0 & 0 & 0 & 1 \\ 0 & 0 & 1 & 0 \end{vmatrix}$$

The two possible superspace groups that are compatible with the observed extinction conditions of $-h+k+l \neq 3n$ for *hklm* and $m \neq 2n$ for *h*0*lm* are $R3m(00\gamma)0s$ and the corresponding centrosymmetric superspace group $R\bar{3}m(00\gamma)0s$. $R\bar{3}m(00\gamma)0s$ was chosen initially and then confirmed by the successful structure solution.

The structure was solved via both a 3-D and a 4-D formalism using JANA2000.[43] Relevant crystallographic information is compiled in Table 1 and Table 2 for the 3-D and 4-D structures, respectively, and the atomic coordinates are given in Table 3 (3-D option) and Tables 4 and 5 (4-D option).

(43) Petricek, V.; Dusek, M. *JANA2000: Programs for Modulated and Composite Crystals*; Institute of Physics: Praha, Czeck Republic, 2000.

Table 1. Crystallographic Data and Structure Refinement for $Sr_6Rh_5O_{15}$ (3-D Option)

formula	$Sr_6Rh_5O_{15}$
formula weight	1280.24
wavelength	Mo Kα ($\lambda = 0.710\ 73$ Å)
space group	*R*32
cell parameters	$a = 9.6517(5)$ Å $b = 9.6517(5)$ Å $c = 13.0480(5)$ Å $\alpha = 90°$ $\beta = 90°$ $\gamma = 120°$
volume	1052.65(8) Å^3
Z	3
density (calc)	6.058 (g/cm^3)
absorption coefficient	28.39 mm^{-1}
twin matix (48/52(3)%)	$\begin{vmatrix} \bar{1} & 0 & 0 \\ 0 & \bar{1} & 0 \\ 0 & 0 & \bar{1} \end{vmatrix}$
F (000)	1719
$2\theta_{max}$	60°
index ranges	$-13 = <h = <13$, $-11 = <k = <11$, $-18 = <l = <16$
reflections collected	11 725
unique reflections	648 ($I > 3\sigma(I)$)
R(int)	0.0722
absorption correction	Gaussian method
T_{min}, T_{max}	0.0671, 0.2373
refinement method	full-matrix least-squares on F^2
data/restraints/parameters	648/0/44
goodness of fit on F^2	2.94
R [$I > 3\sigma(I)$]	0.0317
wR ($w = 1/\sigma^2(F_0)^2$)	0.0661
extinction coefficient	0.059(7)
$(\Delta/\sigma)_{max}$	0.0002

Results and Discussion

Structure. Large black hexagonal rod- or platelike single crystals of $Sr_6Rh_5O_{15}$ ranging in size from submillimeter to ~4 mm in length were grown from a molten potassium carbonate flux. Figure 1 is a SEM image of two crystals obtained from the flux, showing the variability in size and aspect, which can be controlled by adjusting the growth conditions. The SEM also verified the presence of Sr and Rh in all crystals. A large needle-shaped crystal is typically used for the aligned single-crystal magnetic measurements (see below); however, a small crystal was chosen for the structure determination.

Table 2. Crystallographic Data and Structure Refinement for $Sr_6Rh_5O_{15}$ (4-D Option)

formula	$Sr_{1.2}RhO_3$ ($Z = 3$)
cell parameters	$a = 9.6517(5)$ Å $c_1 = 2.6096(3)$ Å $c_2 = 4.3493(1)$ Å $q = 0.6c_1$* $V = 210.53(2)$ Å^3
superspace group	$R\bar{3}m(00\gamma)0s$
twin matrix (47/53(4)%)	$\begin{vmatrix} \bar{1} & 0 & 0 \\ 0 & \bar{1} & 0 \\ 0 & 0 & \bar{1} \end{vmatrix}$
unique reflections	649 ($I > 3\sigma(I)$)
refinement method	F^2
parameters/restraints	32/0
final R values	$R = 0.0411$ ($Rw = 0.0936$) for all reflections $R = 0.0301$ ($Rw = 0.0680$) for 303 main reflections $R = 0.0651$ ($Rw = 0.1335$) for 309 satellites of order 1 $R = 0.1476$ ($Rw = 0.2741$) for 32 satellites of order 2 $R = 0.3447$ ($Rw = 0.8221$) for 5 satellites of order 3
goodness of fit on F^2	4.11
$(\Delta/\sigma)_{max}$	0.0001

Table 3. Atomic Positions and Equivalent Isotropic Displacement Parameters for $Sr_6Rh_5O_{15}$ (3-D Option).

atom	site	x	y	z	U_{eq} (Å^2)
Sr1	9d	0.6757 (1)	0	0	0.0182(4)
Sr2	9e	0.3520(1)	0	$^1/_2$	0.0146(3)
Rh1	6c	0	0	0.90417(8)	0.0071(2)
Rh2	6c	0	0	0.70851(9)	0.0112(3)
Rh3	3b	0	0	$^1/_2$	0.0133(4)
O1	18f	0.1683(8)	0.1622(7)	0.8095(4)	0.019(1)
O2	9d	0.1640(10)	0	0	0.014(3)
O3	18f	0.8480(10)	0.8560(10)	0.6096(5)	0.071(4)

For the 3-D structure determination of $Sr_6Rh_5O_{15}$, the atomic positions of $Sr_6Co_5O_{15}$ were used as the starting positions for the refinement. After several refinement cycles, a final residual factor of $R = 3.17\%$ was obtained for 44 independent refined parameters (Table 1).

For the 4-D structure determination, the structure was solved as a composite structure. As mentioned earlier, this structure type can be considered to be a modulated chain composite structure (commensurate or incommensurate) with two subsystems. In our case, the γ-component of the q vector is $^3/_5$. As described in refs 32 and 33, the $(3 + 1)$-dimensional superspace group gives rise to three possible three-dimensional space groups ($R\bar{3}$, $R32$, and $R3$), as a function of the t-phase section. The t value of $^1/_4$ corresponds to the space group $R32$, which, consequently, was chosen for the refinement of this structure. As proposed in the paper by Perez-Mato et al.,[32] a sawtooth-type function defined by its center ($\hat{x}_4$), its width (Δ),[44,45] and its maximum amplitude for the displacive z-component, was used to describe the atomic positions. To make a valid comparison between the 3-D and the 4-D structure determinations, the number of parameters used for the 4-D structure solution (average atomic positions plus modulations) *must* not exceed the number of parameters used for the 3-D solution. Therefore, the number of variables used in the 4-D refinement must be limited accordingly. For example, in the 3-D model, the strontium atoms occupy two independent positions in the 9d and 9e sites, respectively (Table 3). There are two refineable positional parameters, and therefore, in the 4-D commensurate option, the maximum number of variables used to describe the strontium position should be limited to two. Specifically, in the 4-D structural model utilized,[32] two strontium atoms must be refined: (Sr1) located in the $[Sr_3O_9]$ layer and (Sr2) located in the $[Sr_3RhO_6]$ layer. Since both atoms are located at an average position of (x 0 $^1/_4$), requiring the refinement of one positional variable, x, no positional modulations can be applied in this commensurate model as that would require more than two variables. The same reasoning applies to the rhodium atom occupying the trigonal prismatic site. In the 3-D option, the (Rh3) position is on a special position (0 0 $^1/_2$), which is not refined. Consequently, in the 4-D option the amplitude of the (Rh2) position is zero and the positional modulation, similarly, is not refined. On the other hand, since there are two rhodium octahedral sites in the 3-D structure description, and only one in the 4-D description, it is permissible, in this case, to refine the displacive modulation of the rhodium position to third order. Furthermore, in the 3-D model, there are three positions for the oxygen atoms, which correspond to seven refineable parameters. In the 4-D option, consequently, the atomic modulation functions are refined to third order.

Using these criteria, the structure has been refined, with the results given in Table 2 and the various refined parameters gathered in Tables 4 and 5. The R values are similar to those obtained for the 3-D option. It is important to point out that only 32 parameters needed to be refined in the 4-D option compared to the 44 parameters needed for the 3-D option. A comparison of selected bond distances for the two models is shown in Table 6. It may be noticed that all observed differences fall within the standard deviations of the bond distances.

The structure solutions obtained from the 4-D superspace group formalism and the 3-D approach can, therefore, be considered equivalent. By this example, the efficiency of the 4-D superspace formalism for describing this structural type in a unified form has been demonstrated. Indeed, one can show that if the c-parameter becomes very long, the number of independent atoms in the superstructure and therefore the number of refineable parameters increase significantly for the 3-D structure solution approach. On the contrary, in the superspace formalism, the number of independent atoms is constant, irrespective of the value of the modulation vector q (commensurate or incommensurate). Moreover, the superspace group is always the same and independent of the q value. The accuracy of the results is determined and limited only by the order of the atomic modulation functions introduced in the refinement.

An approximate [110] view of the composite structure of $Sr_6Rh_5O_{15}$ is shown in Figure 2. The repeat sequence in the face-shared polyhedral $[(A',B)O_3]_\infty$ subsystem consists of four consecutive RhO_6 octahedra followed by one distorted RhO_6 trigonal prism. The metal−oxygen bond distances (Rh−O = 1.926(6)−2.069(5) Å) are typical for oxides of this type.[24,25] Intrachain Rh−Rh (2.501(1)−2.721(1) Å) distances can be considered to be nonbonding.

$Sr_6Rh_5O_{15}$ is an $m = 1$, $n = 1$ member of the $A_{3n+3m}A'_nB_{3m+n}O_{9m+6n}$ family. Its synthesis and successful structure determination further establish the validity of the general structural classification developed by Darriet and Subramanian.[31,32] The single-crystal structure of $Sr_6Rh_5O_{15}$ does not have the doubled a-axis, as observed by us in X-ray powder data,[41] nor does it

(44) Petricek, V.; Van der Lee, A.; Evain, M. *Acta Crystallogr.* **1995**, *A51*, 529.

(45) Boucher, F.; Evain, M.; Petricek, V. *Acta Crystallogr.* **1996**, *B52*, 100.

Table 4. Fractional Atomic Average Coordinates, Equivalent Isotropic Displacement Factors, and Atomic Positional and DWF Modulation Coefficients for $Sr_6Rh_5O_{15}$ (4-D Option)[a].

atom	x_0	y_0	z_0	U_{eq} (Å^2)
		Subsystem [(Rh, Rh′)O_3]: $R\bar{3}m(00\gamma)0s$		
Rh1	0	0	0	0.0090(3)
Rh2	0	0	0	0.0131(6)
O	0.1579(5)	0.1579(5)	$^1/_2$	0.028(2)
		Subsystem [Sr]: $P\bar{3}c1(001/\gamma)$		
Sr1	0.3243(2)	0	$^1/_4$	0.0182(7)
Sr2	0.3517(2)	0	$^1/_4$	0.0145(6)
Rh1:	$U^{Rh1}_{z,1} = 0.0016(4)$		$U^{Rh1}_{z,3} = -0.0057(5)$	
	amplitude $= -0.8\,\delta_0/c$	$\hat{x}_4 = {}^1/_4$		$\Delta = 0.4$
	$U^{Rh1}_{U11,2} = U^{Rh1}_{U22,2} = 2U^{Rh1}_{U12,2} = -0.0007(4)$		$U^{Rh1}_{U33,2} = -0.0056(5)$	
Rh2:	amplitude $= 0$	$\hat{x}_4 = {}^1/_4$		$\Delta = 0.1$
O:	$U^{O}_{x,1} = U^{O}_{y,1} = 0.0095(7)$		$U^{O}_{x,2} = -U^{O}_{y,2} = 0.0025(3)$	
	$U^{O}_{x,2} = -0.004(2)$			
	$U^{O}_{x,3} = -U^{O}_{y,3} = -0.0045(4)$		$U^{O}_{z,3} = 0.021(2)$	
	$U^{O}_{x,4} = U^{O}_{y,4} = -0.004(1)$			
	amplitude $= -0.07642 = -\delta_0/c$	$\hat{x}_4 = {}^1/_4$		$\Delta = {}^1/_2$
Sr1:	amplitude $= 0$	$\hat{x}_4 = {}^1/_2$		$\Delta = 0.1667$
Sr2:	amplitude $= 0$	$\hat{x}_4 = 0$		$\Delta = 0.1667$

[a] Modulation functions for a parameter λ of an atom ν defined in a restricted interval are given by the following: $U^{\nu}_{\lambda}(x_4) = \sum_{n=0}^{k} U^{\nu}_{\lambda,n}\mathrm{ortho}^{\nu}_n(x_4)$, where the orthogonalized functions, obtained through a Schmidt orthogonalization routine, are given by $\mathrm{ortho}^{\nu}_i(x_4) = B^{\nu}_0 + \sum_{n=1}^{k} A^{\nu}_n \sin(2\pi n x_4) + \sum_{n=1}^{k} B^{\nu}_n \cos(2\pi n x_4)$ with coefficients B^{ν}_0, A^{ν}_n, B^{ν}_n given in Table 5.

Table 5. Coefficients of the Orthogonalized Functions (4-D Option)

ortho^{o}_i	B^{O}_0	A^{O}_1	B^{O}_1	A^{O}_2	B^{O}_3
ortho^{o}_0	1				
ortho^{o}_1	−2.069	3.249			
ortho^{o}_2	0	0	1.414		
ortho^{o}_3	0	0	−2.271	2.675	
ortho^{o}_4	−2.187	2.785	0	0	1.953
ortho^{Rh1}_i	B^{Rh1}_0	A^{Rh1}_1	B^{Rh1}_1	A^{Rh1}_2	B^{Rh1}_3
ortho^{Rh1}_0	1				
ortho^{Rh1}_1	0	1.616			
ortho^{Rh1}_2	−0.395	0	1.689		
ortho^{Rh1}_3	0	−0.976	0	1.767	
ortho^{Rh1}_4	0.627	0	−1.184	0	1.852

Table 6. Selected Bond Distances for $Sr_6Rh_5O_{15}$ (3-D and 4-D Options)

		distance (Å)		
atom	atom	3-D option	4-D option	
Rh1	O1	2.018(5)	2.016(5)	(×3)
Rh1	O2	2.017(7)	2.012(6)	(×3)
Rh2	O3	1.926(6)	1.940(7)	(×3)
Rh2	O1	2.069(5)	2.084(6)	(×3)
Rh3	O3	2.022(9)	2.023(9)	(×6)
Rh1	Rh1	2.501(1)	2.500(1)	(×1)
Rh1	Rh2	2.553(2)	2.554(2)	(×1)
Rh2	Rh3	2.721(1)	2.720(1)	(×2)

contain any rhodium vacancies, as observed by Gonzalez-Calbet et al.[42] in their powder sample. Clearly, sample preparation is critical and small variations in the synthesis conditions of powders can lead to significant deviations from the ideal structure and composition.[46] This suggests that, for many members of this large family of oxides, structure solutions based on single crystals are preferred and cannot always be compared

(46) Stitzer, K. E.; Henley, W. H.; Claridge, J. B.; zur Loye, H.-C.; Laylard, R. C. *J. Solid State Chem.*, submitted.

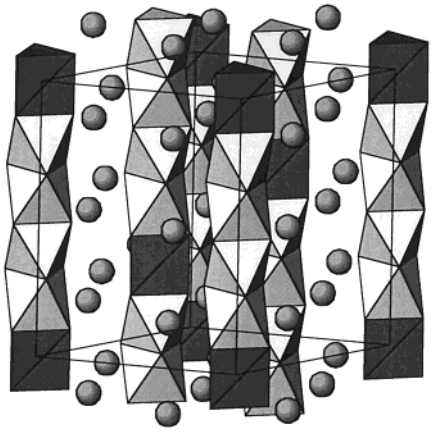

Figure 2. Approximate [110] view of the structure of $Sr_6Rh_5O_{15}$ consisting of chains of four face-sharing RhO_6 octahedra followed by one RhO_6 trigonal prism: light gray, RhO_6 octahedra; dark gray, RhO_6 trigonal prisms; gray spheres, Sr atoms.

to powder structures due to differences in preparation and, potentially, sample composition. In fact, the work by Gonzalez-Calbet[42] supports this last point. It is quite clear that the specific synthesis conditions (oxygen partial pressure, heating rate, temperature, time, precursors, etc.) greatly affect the products that one obtains. Consequently, while an analysis of small crystallites in a powder sample is undoubtedly reasonable, it is not assured that such information can be used to extrapolate to samples made under different synthesis conditions and certainly not to other compositions. In fact, a very cautious and conservative approach would be to consider each powdered sample, containing metals that can take on multiple oxidation states, as a unique composition with a unique structure and concomitant properties.

Five compounds isostructural with $Sr_6Rh_5O_{15}$, where crystal structures have been published, include $Ba_6Ni_5O_{15}$,[11] $Sr_6Co_5O_{15}$,[12] $Ba_6CuIr_4O_{15}$,[13] and $Ba_6Mn_4MO_{15}$ (M = Cu, Zn).[47] All of the structures consist of a polyhedral chain repeat sequence of four face-sharing octahedra followed by one trigonal

prism. In the case of $Ba_6Ni_5O_{15}$, $Sr_6Rh_5O_{15}$, and $Sr_6Co_5O_{15}$, both polyhedral sites, i.e., the octahedra and the trigonal prism, are occupied by the same atom type; however, for the other compounds, the sites are occupied by the two different metal atoms. Potential oxidation states for nickel in $Ba_6Ni_5O_{15}$ include Ni^{2+}, Ni^{3+}, and Ni^{4+}.[11] No assignment of oxidation states was proposed for cobalt in $Sr_6Co_5O_{15}$, for which the average oxidation state +3.6.[12] Potential oxidation-state distributions for rhodium in $Sr_6Rh_5O_{15}$ include three Rh^{4+} and two Rh^{3+}. One might expect that the location of the Rh^{3+} and Rh^{4+} cations in the chain could be obtained from Rh−O bond lengths using, for example, the bond valence approach. However, in this case, it turns out that the average metal−oxygen bond lengths for all the polyhedra are essentially identical within experimental error. Consequently, it is not possible to make an assignment of oxidation states by this approach, and further clarification will have to await planned neutron diffraction and XANES experiments.

Magnetism. The availability of large single crystals presents a great opportunity to carry out magnetic measurements on oriented single crystals. While there exists an extensive literature on anisotropic magnetic materials and the determination of their magnetic behavior using single crystals,[1,2] this is typically not the case for this family of oxides. Anisotropies have been predicted for these pseudo-one-dimensional materials, and the most in-depth investigations have been carried out on $Ca_3Co_2O_6$, an $n = 1$, $m = 0$ member of this family, using polycrystalline samples[48,49] and, more recently, single crystals.[50] The work on single crystals confirmed the magnetic structure as consisting of a triangular lattice of ferromagnetic $[Co_2O_6]$ chains that are coupled antiferromagnetically. Other systems include Sr_3NiPtO_6, where magnetic susceptibility studies on oriented single crystals indicate the presence of Ni(II) ions with a large single-ion anisotropy.[4] $Sr_6Rh_5O_{15}$ is the latest oxide of this family for which large crystals have been grown and where, consequently, it is possible to carry out such experiments.

For comparison, powder susceptibility measurements were carried out on a sample of finely ground single crystals of $Sr_6Rh_5O_{15}$. The magnetic susceptibility and inverse susceptibility as a function of temperature for such a randomly oriented polycrystalline sample is shown in Figure 3. The susceptibility curve increases to a maximum at 11 K, followed by a decrease in the susceptibility, indicative of antiferromagnetic correlations.

Single-crystal magnetic measurements were performed using a large single crystal, 3.0 mm in length and weighing 1.88(1) mg. Though unsuitably large for a single-crystal structure determination, the crystal system and unit cell parameters of this crystal were determined on a Bruker SMART APEX CCD single-crystal diffractometer after the magnetic measurements were performed and shown to be identical to those used for the structure solution. The crystal was affixed to a Quantum Design crystal rotator device and immersed in the SQUID magnetometer. The crystal rotator enables continuous in situ measurements of the magnetization as a function of crystal orientation relative to the applied field. Figure 4 plots the magnetic susceptibility of the single crystal as a function of crystal orientation at 2 K. A regular sinusoidal variation in the susceptibility is clearly evident. The maximums in the susceptibility correspond to a

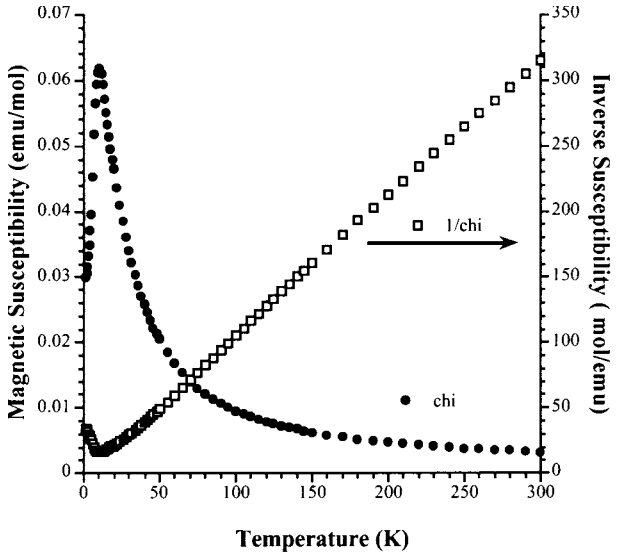

Figure 3. Temperature dependence of the magnetic susceptibility (closed circles) and the inverse susceptibility (open squares) of $Sr_6Rh_5O_{15}$ powder at 5 kG.

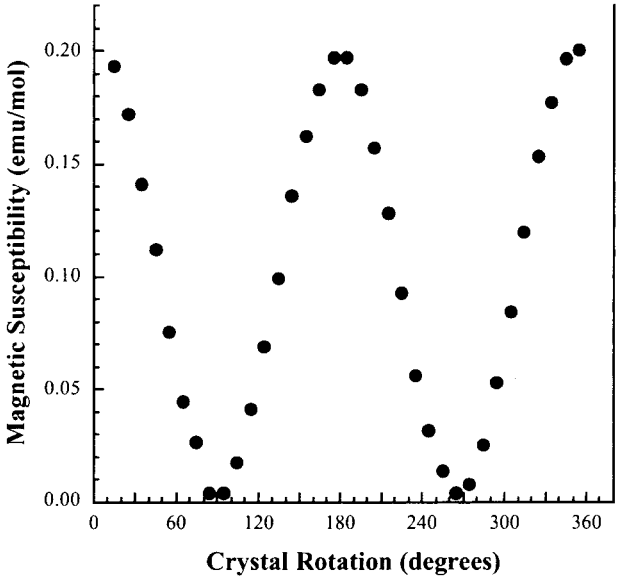

Figure 4. Magnetic susceptibility of a single crystal of $Sr_6Rh_5O_{15}$ as a function of crystal orientation with respect to the applied magnetic field measured at 11 K and 5 kG. The maximums occur for the crystal *c*-axis aligned parallel with the applied field.

parallel alignment of the hexagonal *c*-axis (i.e., the $[Rh_5O_{15}]_\infty$ chain direction) with the applied field and the minimums correspond to a 90° rotation from that position or a perpendicular orientation of the *c*-axis relative to the magnetic field. A large magnetic anisotropy is clearly evident, with a ratio of *M*(parallel)/M(perpendicular) $\sim$ 40 at 11 K. Interestingly, the minimum is virtually zero, considering experimental uncertainties due to the rotator background subtraction. The strength of this collinear arrangement is demonstrated by Figure 5, which shows the temperature dependence of the magnetic susceptibility of the single crystal as a function of crystal alignment. It can be seen that the magnetic anisotropy persists all the way up to room temperature and beyond, as shown in Figure 6, which shows the magnetic anisotropy as a function of temperature. It is worth noting that the magnetic correlations are evident only for the crystal in the parallel orientation and essentially absent for the

(47) Cussen, E. J.; Vente, J. F.; Battle, P. D. *J. Am. Chem. Soc.* **1999**, *121*, 3958.
(48) Kageyama, H.; Yoshimura, K.; Kosuge, K.; Azuma, M.; Takano, M.; Mitamura, H.; Goto, T. *J. Phys. Soc. Jpn.* **1997**, *66*, 3996.
(49) Aasland, S.; Fjellvag, H.; Hauback, B. *Solid State Commun.* **1997**, *101*, 187.
(50) Maignan, A.; Michel, C.; Masset, A. C.; Martin, C.; Raveau, B. *Eur. Phys. J.* **2000**, *B15*, 657.

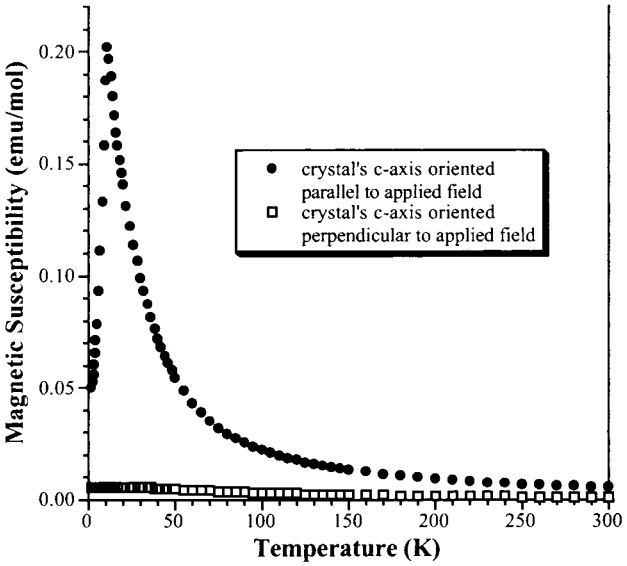

Figure 5. Temperature dependence of the magnetic susceptibility of a single crystal of $Sr_6Rh_5O_{15}$ oriented parallel (closed circles) and perpendicular (open squares) with respect to the applied field of 5 kG.

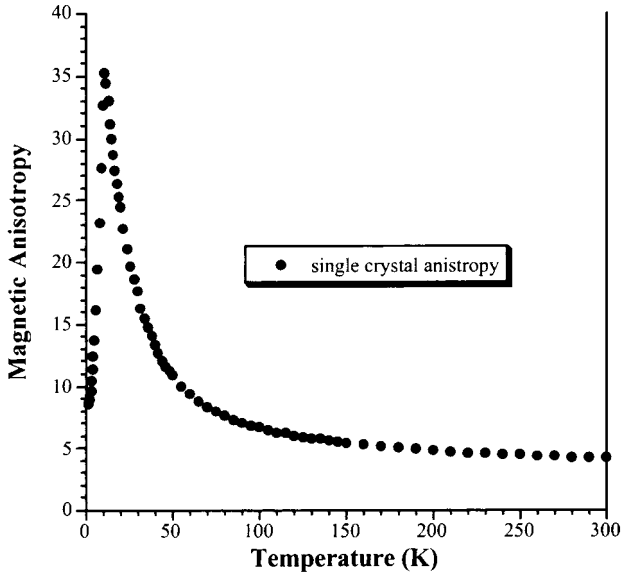

Figure 6. Temperature dependence of the magnetic anisotropy (defined as the ratio between the susceptibility of a single crystal of $Sr_6Rh_5O_{15}$ oriented parallel and perpendicular with respect to the applied field) measured at 5 kG.

perpendicular orientation. This suggests that the antiferromagnetic correlations are strongly coupled to the chain direction.

These measurements demonstrate the importance of carrying out magnetic measurements on single crystals, at least for this rhodium family of oxides. Previous measurements performed on powdered samples[41] necessarily yielded an averaged result. For this material, since the magnetization in one direction is effectively zero, we would expect the powder average to be one-third of the maximum single crystal value. Figure 7 compares the powder susceptibility measured on a randomly oriented polycrystalline sample of $Sr_6Rh_5O_{15}$ (obtained by grinding a sample of single crystals to a fine powder) with that of the single crystal. The powder data are multiplied by a factor of 3 to reflect the random orientation of the crystallites. The data overlay quite well, demonstrating that the powder value is indeed a random average of the various crystal orientations. It also suggests that magnetic measurements carried out on random powders of oxides in this family may represent only a powder average, the exact value of which would depend on the magnitude of the magnetic anisotropy that each *randomly oriented crystallite* is displaying and on the temperature at which it is measured, since the anisotropy has a temperature dependence (Figure 6). Although the existence of such an anisotropy has been hypothesized previously in several members of this family, including Sr_3CuIrO_6,[51] it has now become possible to demonstrate its existence. It is also clear that this large magnetic anisotropy is not unique to $Sr_6Rh_5O_{15}$, as similar results have been observed in other oxide members of this family.[50,52]

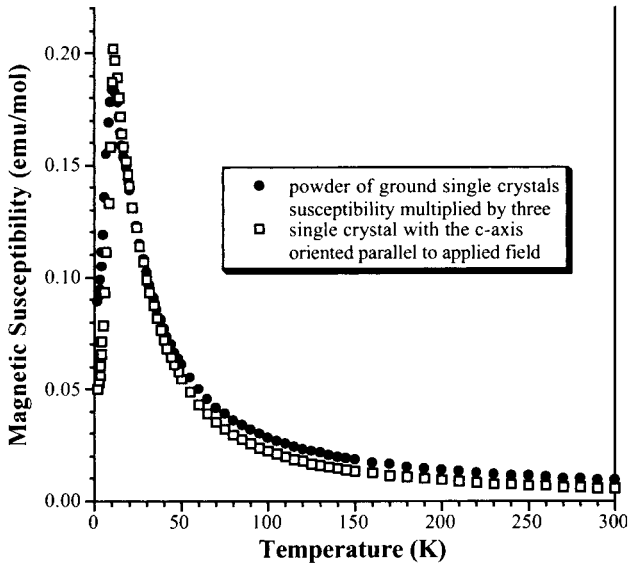

Figure 7. Correlation between the magnetic susceptibility of a single crystal of $Sr_6Rh_5O_{15}$ (open squares), oriented parallel to the applied field of 5 kG and the susceptibility of $Sr_6Rh_5O_{15}$ powder (closed circles) multiplied by a factor of 3, measured at 5 kG.

Acknowledgment. Financial support from the National Science Foundation through Grant DMR: 9873570 is gratefully acknowledged.

Supporting Information Available: An X-ray crystallographic file is available in CIF format: tables of crystal data and refinement information as well as of fractional atomic coordinates and displacement factors of the atoms and the modulation coefficients. This material is available free of charge via the Internet at http://pubs.acs.org. See any current masthead page for ordering information and Web access instructions.

JA011071G

(51) Nguyen, T. N.; zur Loye, H.-C. *J. Solid State Chem.* **1995**, *117*, 300.

(52) zur Loye, H.-C.; Stitzer, K. E.; Smith, M. D.; El Abed, A.; Darriet, J. *Inorg. Chem.*, in press.